Annals of Glaciology 37 2003

A dislocation-based analysis of the creep of granular ice: preliminary experiments and modeling

David M. COLE
U.S. Army Cold Regions Research and Engineering Laboratory, 72 Lyme Road, Hanover, NH 03755-1290, U.S.A.
E-mail: dmcole@crrel.usace.army.mil

ABSTRACT. The nature of the fall-off at lower stresses from power-law behavior to a lower-order stress dependency is of particular interest in glacier and ice-sheet modeling. Preliminary experiments show that the stress level at which the fall-off occurs is a function of the specimen's dislocation density. The analysis employs a dislocation-based model of anelasticity that provides a quantitative relationship between the effective dislocation density and the area of hysteresis loops observed in cyclic loading experiments. Combining this technique with a staged creep experiment makes it possible to calculate the dislocation density as a function of strain, thereby supporting a quantitative dislocation analysis of the deformation process. Work on saline ice established that the threshold stress associated with power-law behavior increased as a result of prior straining, power-law behavior emerged when the effective dislocation density increased measurably during deformation, and approximately linear behavior was evident when the dislocation density remained relatively constant. Those findings motivated the experiments on fresh-water ice presented here. The preliminary experiments show that pre-straining increases the stress associated with the fall-off from power-law behavior, and the results are interpreted in the context of a dislocation-based constitutive model developed for sea ice.

INTRODUCTION

The observation that experiments on ice frequently show a fall-off to a lower-order stress dependency at low stress is of particular interest because of the relevance of this stress regime to glacier and ice-sheet modeling. Analyses of large-scale ice masses indicate that an $n = 3$ flow law underpredicts flow rates at low stresses (e.g. Cuffey and others, 2000a,b; Peltier and others, 2000), and alternative models that predict a fall-off from power-law behavior are currently being sought.

Laboratory data on granular fresh-water ice frequently show a fall-off to a lower-order stress dependence at low stresses (Langdon, 1973), and recent work on saline ice (Cole and Durell, 2001) demonstrated that the stress associated with this fall-off is a function of dislocation density. Because of the implications for the field of glaciology, preliminary experiments were conducted on several specimens of granular fresh-water ice. The results show that increasing a specimen's dislocation density by pre-straining brings about a deviation from power-law behavior, as observed in saline ice. The paper also presents data for saline ice that demonstrate the validity of the staged-creep methodology. The results are evaluated in the context of a dislocation-based constitutive model.

BACKGROUND

A good deal of experimental data indicate that previously unstrained polycrystalline ice subjected to unconfined compression, having grain-sizes typically found in ice sheets, generally exhibit $n \approx 3$ power-law creep behavior (e.g. Barnes and others, 1971; Jacka, 1984). Unconfined compression data can produce $3 < n \leq 4$ if the dataset extends above $\approx 10^{-6}\ \mathrm{s}^{-1}$, primarily due to microcracking effects (Cole, 1986). Barnes and others (1971, fig. 2) and Goldsby and Kohlstedt (2001, fig. 1) clearly show the break in slope associated with the onset of cracking. On the other hand, n values of ≈ 4 emerge in experiments at pressures over ≈ 30 MPa (Kirby and others, 1987; Durham and others, 1992), accompanied by a relatively high, negative activation volume. As pointed out by Weertman (1968, 1983), $n = 3$ behavior can result from drag- or diffusion-controlled processes, although the dislocation configuration needed for diffusion-controlled $n = 3$ behavior appears less likely for ice, and $n = 4$ behavior can be explained by diffusion-controlled processes.

Although there is still some uncertainty regarding activation volumes for specific processes in ice, there is reasonable support for associating diffusion-based processes with large negative activation volumes (Azuma and Higashi, 1983; Hondoh and others, 1987), and drag-controlled processes with small, positive activation volumes (Taubenberger and others, 1973; Cole, 1996). The confined creep experiments of Jones and Chew (1983) indicate a shift to a large negative activation volume at a confining pressure of ≈ 30 MPa. That finding supports flow models with diffusion-based rate-controlling processes (e.g. Fukuka and others, 1987; Castelnau and others, 1997) for pressures above ≈ 30 MPa. However, below 30 MPa, Jones and Chew's (1983) results indicated a mechanism shift. Specifically in the experiments where pressure was varied on individual specimens, pressure had a minimal effect on the creep rate, with a slight trend toward a positive activation volume. That behavior is commensurate with the drag-controlled process

https://doi.org/10.3189/172756403781815564 Published online by Cambridge University Press

that forms the basis of the model of Cole and Durell (2001). Additionally, that work showed that the dislocation density ρ is proportional to σ^2, with a temperature dependence of $Q_\rho = 0.45$ eV. This leads to an increase in the apparent activation energy of creep when dislocation multiplication occurs, in keeping with experimental observations on fresh-water ice (Weertman, 1983).

Goldsby and Kohlstedt (1997, 2001) employed unique specimen preparation methods to explore the mechanics of extremely small (<0.2 mm) grain-sized fresh-water ice specimens. They found regimes of $n = 2.4$, 1.8 and 4.0, which were identified, respectively, as basal slip-accommodated grain boundary sliding, grain boundary sliding-accommodated basal slip, and dislocation creep regimes. As articulated in the associated model, grain boundary diffusion is expected to be important even at low pressure given the small grain-sizes of that material. Since grain growth, which typically results in a low dislocation density, was used to produce their larger-grained material, the possibility exists that the initial dislocation density in those specimens varied substantially with grain-size. As demonstrated in the work presented below, that circumstance could have a profound effect on the material's constitutive behavior.

The present effort was motivated by a combined creep and cyclic loading experiment on an Arctic sea-ice core (Cole and Durell, 2001) that followed an $n = 3$ power-law behavior when subjected to an initial set of increasing creep stresses, but followed an approximately linear stress dependence upon reloading at lower stress levels. The dislocation density increased when power-law behavior was observed, and remained virtually constant when approximately linear behavior was observed. Those experiments also revealed that the viscous strain rate varied directly with the effective dislocation density.

METHODS

The experiments begin with the application of cyclic loading (sets of 10^{-1} Hz sine waves), followed by alternating periods of uniaxial creep and cyclic loading. The motion of the mobile dislocations under cyclic loading produces a loss compliance that can be calculated from the loop area (Cole, 1995). The associated relaxation strength δD^d is related to the dislocation density ρ (m^{-2}):

$$\delta D^d = \frac{\rho \Omega b^2}{K} . \qquad (1)$$

Ω is an orientation factor that determines the average basal plane shear stress from the background normal stress ($\Omega = 0.32$ for randomly oriented grains). b is Burgers vector (4.52×10^{-10} m), and K is the experimentally determined restoring stress constant (0.07 Pa).

Table 1 shows the cyclic and creep loading histories for each specimen, along with the accumulated strains. At the end of each period (or stage) of creep loading, the viscous and anelastic (creep recovery) components of strain were determined. The average viscous strain rate was calculated by dividing the viscous strain by the time under load. This method eliminates transient effects from the strain-rate calculation. The accumulated strain levels were kept relatively low in these experiments to minimize microstructural changes. Additionally, Cole and Durell (1995) established that the cyclic loading employed here does not change the dislocation density, and given the observations of Cole (1986) on granular ice, microcracking is unlikely to have an influence on the present observations. As shown below, the staged-creep method can be used to examine the stress–strain-rate relationship on a single specimen.

Table 1. Cyclic and staged creep loading history. $T = -10°C$ for all experiments

Specimen	*Cyclic stress levels*	*Creep loading stage*			
		Initial loading		*Subsequent loading*	
		Stress	*Accumulated strain*	*Stress*	*Accumulated strain*
	MPa	MPa		MPa	
HO730	±0.2, 0.4	−2.0	4.305×10^{-3}	−0.2	4.308×10^{-3}
				−0.6	4.55×10^{-3}
				−1.0	4.98×10^{-3}
				−1.4	5.86×10^{-3}
HO73	±0.2, 0.4	−2.0	4.62×10^{-3}	−0.4	4.65×10^{-3}
				−0.8	4.85×10^{-3}
				−1.2	5.16×10^{-3}
				−1.6	6.02×10^{-3}
NP611	±0.2, 0.4, 0.6, 0.8	−0.2	8.29×10^{-4}	−0.2	1.57×10^{-3}
		−0.4	3.07×10^{-4}	−0.4	1.68×10^{-3}
		−0.6	7.45×10^{-4}	−0.6	1.91×10^{-3}
		−0.8	8.74×10^{-4}	−0.8	3.01×10^{-3}
APX1	±0.2, 0.4, 0.6, 0.8, 1.0	−2.5	1.84×10^{-5}	−2.5	2.16×10^{-4}
				−2.5	3.79×10^{-3}

The specimens were granular fresh-water ice prepared by the method of Cole (1979), and measured 127 mm in length and 50.4 mm in diameter. Grain size was 3–5 mm. The cyclic (tension/compression) loading was made possible by the gripping system described in Cole and Gould (1990). All experiments were conducted at $T = -10 \pm 0.1\,°\mathrm{C}$. Strain was calculated from the output of specimen-mounted linear variable displacement transducers.

RESULTS AND DISCUSSION

Figure 1 shows example results for staged creep experiments on three laboratory-prepared saline ice specimens. Note that even though a strain of 0.005 was applied in each stage, $n \approx 3$ power-law behavior was observed. Figure 2 shows representative results for the granular fresh-water ice. The relatively constant hysteresis loop area after the initial loading stage indicates that the mobile dislocation density remained essentially constant for the subsequent stages. Figures 3 and 4 plot the calculated dislocation density vs accumulated viscous strain, and the viscous strain rate vs stress for the indicated specimens. The salient features of the results are:

1. The average as-grown dislocation density was $5.4 \pm 1.4 \times 10^8\ \mathrm{m}^{-2}$.
2. The dislocation density stabilized at a viscous strain level of $\approx 2 \times 10^{-3}$.
3. Two specimens that were pre-strained at −2.0 MPa achieved approximately the same dislocation density.
4. Upon subsequent deformation, pre-strained specimens exhibited increases in:
   a. The stress associated with the fall-off from the $n = 3$ power law
   b. Viscous strain rate for a given creep stress.

https://doi.org/10.3189/172756403781815564 Published online by Cambridge University Press

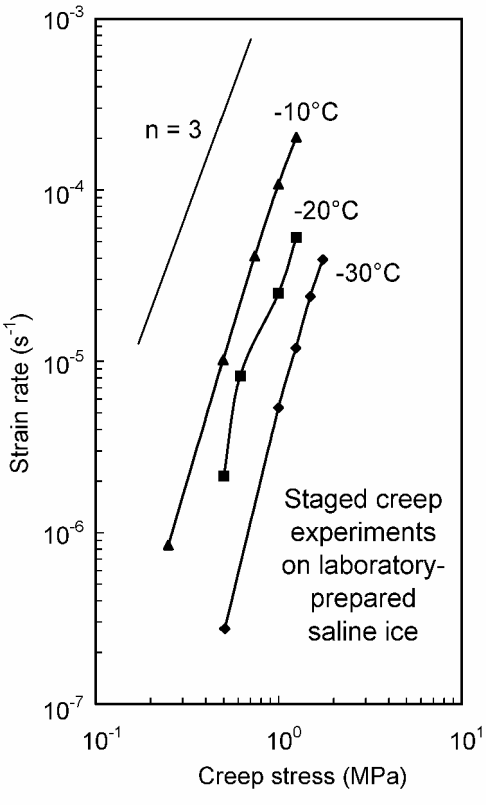

Fig. 1. Strain rate vs stress for staged creep experiments on three laboratory-prepared saline ice specimens. Each data point was obtained during a single stage of the creep test.

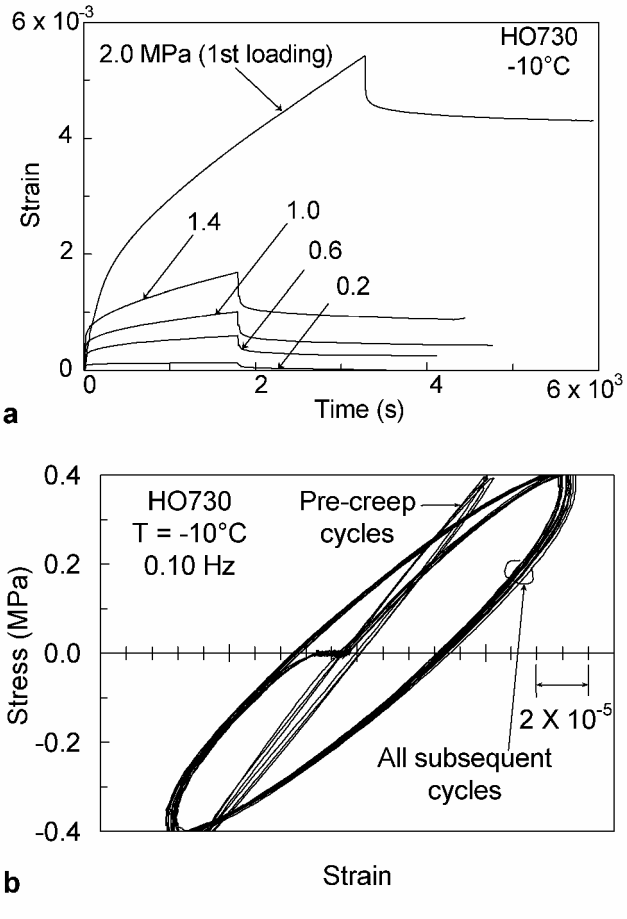

Fig. 2. Creep and cyclic loading responses of specimen HO730. (a) Stress vs time for the five creep loading segments. The stress and loading sequence are indicated. (b) Cyclic loading response to the ±0.4 MPa stress.

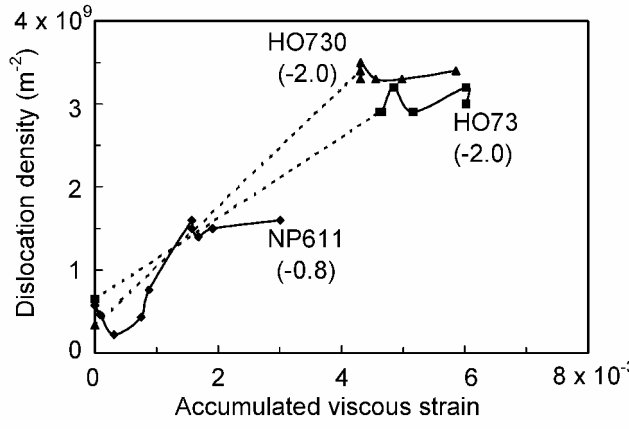

Fig. 3. Calculated dislocation density vs accumulated viscous strain for specimens HO73, HO730 and NP611. The maximum creep stress levels appear in parentheses.

5. The creep recovery strain was linear with stress when the dislocation density remained constant, and non-linear when the dislocation density increased, during deformation.

Analogous to earlier observations on sea ice, the observations indicate that the fall-off from power-law behavior is a function of the specimen's dislocation density and not an intrinsic material property. Significantly, ice in nature can develop relatively high dislocation densities: $>10^{10}$ m^{-2} was observed by Baker and Cullen (2002) in a 94 m Greenland Ice Sheet Project 2 (GISP2) core. J. Kipfsthul and others (unpublished information) have observed extensive slip-band formation in deeper cores, and note that the bands fade in time after removal from the sheet. Dislocation processes are thus clearly active at glaciological time-scales. Although recovery (which reduces the dislocation density) after unloading has been observed in the laboratory (Cole and Durell, 2001), the above observations indicate that naturally deforming ice can sustain substantial dislocation densities. On the other hand, recrystallization would produce regions with low dislocation density that would exhibit $n = 3$ to lower stresses than high-dislocation-density material. Additionally, factors such as impurity or particulate content could result in high dislocation densities irrespective of deformation history. This circumstance would increase the stress associated with the fall-off from $n = 3$ behavior in the same manner as when a high dislocation density is achieved by pre-strain.

The observation that the creep recovery strain varies non-linearly with stress when the dislocation density increases, and linearly when the dislocation density is constant, is commensurate with the dislocation-based interpretation of the constitutive behavior. Additionally, the present results suggest that scatter in the stress level associated with the fall-off from power-law behavior could be due to variations in initial dislocation density.

Cole and Durell (2001) developed a dislocation drag model for sea ice:

$$\dot{\varepsilon}_{\mathrm{visc}} = \frac{\beta\rho\Omega^{3/2}b^2\sigma_{\mathrm{creep}}}{B_0}\exp\left(-\frac{Q_{\mathrm{glide}}}{kT}\right). \qquad (2)$$

β is a numerical constant = 0.3 for sea ice. Q_{glide} is the activation energy for basal glide (0.54 eV). The net stress exponent and apparent activation energy are determined by the extent to which the dislocation density increases during straining. Equation (2) predicts a linear stress dependence

https://doi.org/10.3189/172756403781815564 Published online by Cambridge University Press

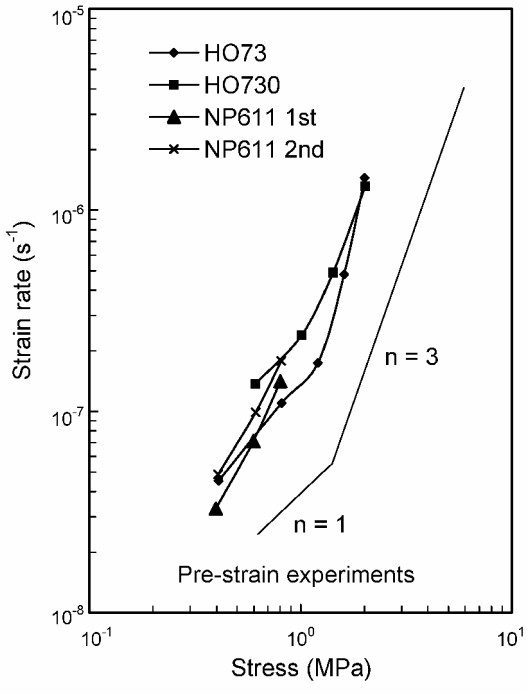

Fig. 4. Log–log plots of strain rate vs stress for laboratory-prepared granular fresh-water ice specimens. HO73 and HO730 experienced −2.0 MPa stress during pre-straining, and NP611 experienced stresses ranging from −0.2 to −0.8 MPa during two loading series.

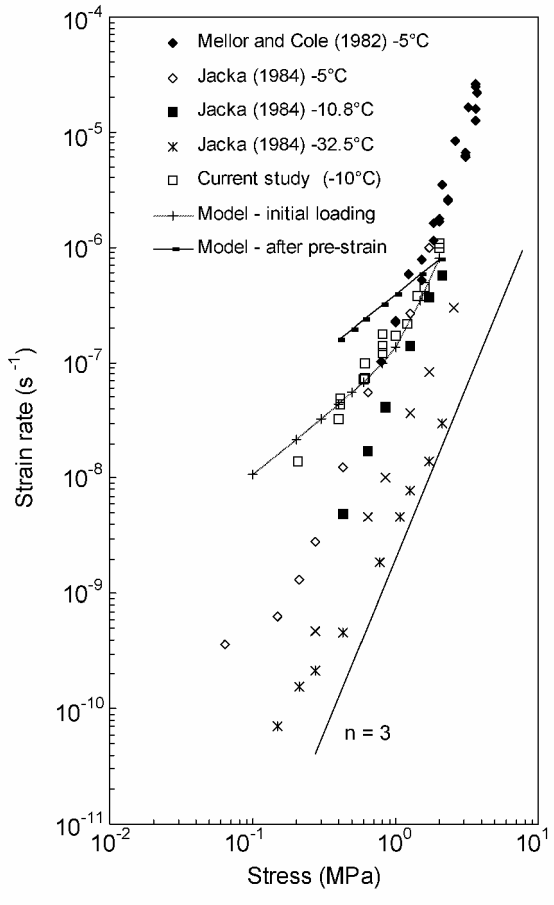

Fig. 5. Preliminary model calculations of strain rate vs stress for initial dislocation densities of 5.4×10^8 m^{-2} (initial loading) and 3.2×10^9 m^{-2} (after pre-strain).

if the dislocation density remains constant, but n increases from 1 to 3 as the dislocation density increases during deformation.

Preliminary calculations indicated that the sea-ice formulation for dislocation density as a function of stress (Cole and Durell, 2001) over-predicted the dislocation density observed for granular fresh-water ice by a factor of ≈2.5. This was not unexpected given the generally high dislocation densities observed in saline ice. It is nonetheless useful to demonstrate that the model is capable of capturing pre-strain effects. Figure 5 shows model predictions of strain rate vs applied stress based on the average initial dislocation density of the present specimens (5.2×10^8 m^{-2}), along with data from the literature. Several points are evident from Figure 5. The model predictions agree with the data from the literature once $n = 3$ behavior is established. The slope of the curve labeled "initial loading" gradually increases because of the magnitude of the initial dislocation density. A smaller value would produce $n = 3$ behavior to lower stresses. The curve labeled "after pre-strain" shows the behavior based on the dislocation density of 3.2×10^9 m^{-2} that was calculated for the pre-strain experiments. While over-predicting the observed values, the model brackets the observations and captures the general trend of higher strain rates and a lower slope evident in the pre-strained specimens.

It is noted that the model is based on sea-ice data and, apart from applying the above-mentioned factor of 2.5 in the dislocation-density–stress relationship, was not otherwise adjusted. It is anticipated that the stress– and perhaps the strain–dislocation-density relationships determined for sea ice will be subject to revision based on the results of a current experimental program on granular fresh-water ice.

CONCLUSIONS

For the stated ice types and experimental conditions, the foregoing results and analysis lead to the following conclusions:

1. The cyclic loading response is sensitive to the deformation history of ice specimens and can be used to determine a calculated dislocation density.
2. Staged creep experiments on a single specimen yield useful information on the strain-rate–stress relationship.
3. Experimental results indicate that the stress level associated with the fall-off from power-law behavior increases with dislocation density.
4. The results of pre-strain experiments on granular fresh-water ice are in general agreement with similar experiments on sea ice.
5. A dislocation drag-based constitutive model is capable of capturing the observed pre-strain effects.

ACKNOWLEDGEMENTS

The author gratefully recognizes the current support of the Arctic Natural Sciences Program (NSF-OPP grant No. 0117371) for this effort, and previous support from the U.S. Army Cold Regions Research and Engineering Laboratory's AT24 basic research program. The outstanding talents of G. Durell, who conducted the laboratory experiments, are also gratefully acknowledged.

https://doi.org/10.3189/172756403781815564 Published online by Cambridge University Press

REFERENCES

Azuma, N. and A. Higashi. 1983. Effects of hydrostatic pressure on the rate of grain growth in Antarctic polycrystalline ice. *J. Phys. Chem.*, **87**(21), 4060–4064.

Baker, I. and D. Cullen. 2002. The structure and chemistry of 94 m Greenland Ice Sheet Project 2 ice. *Ann. Glaciol.*, **35**, 224–230.

Barnes, P., D. Tabor and J. C. F. Walker. 1971. The friction and creep of polycrystalline ice. *Proc. R. Soc. London, Ser. A*, **324**(1557), 127–155.

Castelnau, O., G. R. Canova, R. A. Lebensohn and P. Duval. 1997. Modelling viscoplastic behavior of anisotropic polycrystalline ice with a self-consistent approach. *Acta Mater.*, **45**(11), 4823–4834.

Cole, D. M. 1979. Preparation of polycrystalline ice specimens for laboratory experiments. *Cold Reg. Sci. Technol.*, **1**(2), 153–159.

Cole, D. M. 1986. Effect of grain size on the internal fracturing of polycrystalline ice. *CRREL Rep.* 86-5.

Cole, D. M. 1995. A model for the anelastic straining of saline ice subjected to cyclic loading. *Philos. Mag. A*, **72**(1), 231–248.

Cole, D. M. 1996. Observations of pressure effects on the creep of ice single crystals. *J. Glaciol.*, **42**(140), 169–175.

Cole, D. M. and G. D. Durell. 1995. The cyclic loading of saline ice. *Philos. Mag. A*, **72**(1), 209–229.

Cole, D. M. and G. D. Durell. 2001. A dislocation-based analysis of strain history effects in ice. *Philos. Mag. A*, **81**(7), 1849–1872.

Cole, D. M. and L. D. Gould 1990. Reversed direct-stress testing of ice: equipment and example results. *Cold Reg. Sci. Technol.*, **18**(3), 295–302.

Cuffey, K. M., H. Conway, A. Gades, B. Hallet, C. F. Raymond and S. Whitlow. 2000a. Deformation properties of subfreezing glacier ice: role of crystal size, chemical impurities, and rock particles inferred from in situ measurements. *J. Geophys. Res.*, **105**(B12), 27,895–27,915.

Cuffey, K. M., T. Thorsteinsson and E. D. Waddington. 2000b. A renewed argument for crystal size control of ice-sheet strain rates. *J. Geophys. Res.*, **105**(B12), 27,889–27,894.

Durham, W. B., S. H. Kirby and L. A. Stern. 1992. Effects of dispersed particulates on the rheology of water ice at planetary conditions. *J. Geophys. Res.*, **97**(E12), 20,883–20,897.

Fukuda, A., T. Hondoh and A. Higashi. 1987. Dislocation mechanisms of plastic deformation of ice. *J. Phys.* (Paris), **48**, Colloq. C1, 163–173. (Supplément au 3.)

Goldsby, D. L. and D. L. Kohlstedt. 1997. Grain boundary sliding in fine-grained ice I. *Scripta Mater.*, **37**(9), 1399–1406.

Goldsby, D. L. and D. L. Kohlstedt. 2001. Superplastic deformation of ice: experimental observations. *J. Geophys. Res.*, **106**(B6), 11,017–11,030.

Hondoh, T., K. Azuma and A. Higashi. 1987. Self-interstitials in ice. *J. Phys.* (Paris), **48**, Colloq. C1, 183–186. (Supplément au 3.)

Jacka, T. H. 1984. The time and strain required for development of minimum strain rates in ice. *Cold Reg. Sci. Technol.*, **8**(3), 261–268.

Jones, S. J. and H. A. M. Chew. 1983. Creep of ice as a function of hydrostatic pressure. *J. Phys. Chem.*, **87**(21), 4064–4066.

Kirby, S. H., W. B. Durham, M. L. Beeman, H. C. Heard and M. A. Daley. 1987. Inelastic properties of ice Ih at low temperatures and high pressures. *J. Phys.* (Paris), **48**(3), Colloq. C1, 227–232. (Supplément au 3.)

Langdon, T. G. 1973. Creep mechanisms in ice. *In* Whalley, E., S. J. Jones and L. W. Gold, *eds. Physics and chemistry of ice*. Ottawa, Ont., Royal Society of Canada, 357–361.

Mellor, M. and D. M. Cole. 1982 Deformation and failure of ice under constant stress or constant strain rate. *Cold Regions Science and Technology*, **5**(3), 201–219.

Peltier, W. R., D. L. Goldsby, D. L. Kohlstedt and L. Tarasov. 2000. Ice-age ice-sheet rheology: constraints from the Last Glacial Maximum form of the Laurentide ice sheet. *Ann. Glaciol.*, **30**, 163–176.

Taubenberger, R., M. Hubmann and H. Granicher. 1973. Effect of hydrostatic pressure on the dielectric properties of ice Ih single crystals. *In* Whalley, E., S. J. Jones and L. W. Gold, *eds. Physics and chemistry of ice*. Ottawa, Ont., Royal Society of Canada, 194–198.

Weertman, J. 1968. Dislocation climb theory of steady-state creep. *Am. Soc. Metals Trans.*, **61**, 681–694.

Weertman, J. 1983. Creep deformation of ice. *Annu. Rev. Earth Planet. Sci.*, **11**, 215–240.